IEEE Access
Multidisciplinary ⋮ Rapid Review ⋮ Open Access Journal

Received June 11, 2021, accepted July 7, 2021, date of publication July 21, 2021, date of current version August 9, 2021.

Digital Object Identifier 10.1109/ACCESS.2021.3099006

Genetic Algorithm Based Parameter Tuning for Robust Control of Launch Vehicle in Atmospheric Flight

JOSÉ PABLO BELLETTI ARAQUE, ALESSANDRO ZAVOLI, DOMENICO TROTTA, AND GUIDO DE MATTEIS

Department of Mechanical and Aerospace Engineering, Sapienza - University of Rome, 00184 Rome, Italy

Corresponding author: Alessandro Zavoli (alessandro.zavoli@uniroma1.it)

ABSTRACT A hybrid approach to the design of the attitude control system for a launch vehicle (LV) in the atmospheric flight phase is proposed in this paper, where a structured $\mathcal{H}_\infty$ controller is tuned using a genetic algorithm (GA). The $\mathcal{H}_\infty$ synthesis relies on a classical architecture for the thrust vector control (TVC) system that features proportional-derivative loops and bending filters. Once a set of requirements on stability and robustness typical of industrial practice is specified, control design is carried out by parameterizing the $\mathcal{H}_\infty$ weighting functions, and solving a two-layer max-min global optimization problem for the tuning parameters. The design methodology is applied to the model of a medium-size LV. The novel design is analyzed in off-nominal conditions taking into consideration model parameter scattering and wind disturbances. The results show that the automated design procedure allows to devise time-scheduled controllers providing adequate stability and performance, and appears as a viable and effective solution in order to reduce the burden of recurrent activities for controller tuning and validation conducted prior to each launch.

INDEX TERMS Robust control, genetic algorithm, launch vehicle, attitude dynamics.

I. INTRODUCTION

This paper deals with a hybrid control synthesis technique based on a combination of genetic algorithm (GA) and structured $\mathcal{H}_\infty$ in order to design a robust controller for a launch vehicle (LV) in atmospheric flight. LV attitude control is a challenging engineering problem due to nonlinear dynamics, rapidly changing inertial and aero-propulsive properties, and non-negligible elastic-body deformations [1]. Moreover, typical LV configurations are aerodynamically unstable and, at the same time, the control authority is limited to small aerodynamic surfaces or, more frequently, to the gimbal deflection of a non-throttleable engine, whose angular range is of the order of a few degrees.

Attitude control is required to stabilize the system, reject wind disturbances, and limit transverse loads while minimizing displacement from the reference trajectory. Robustness of the control system to uncertainty on vehicle aero-mechanical parameters, such as bending modes characteristics (namely, natural frequencies and modal participation factors), aerodynamic coefficients, engine exhaust velocity, and gimbal dynamics, is also mandatory.

The associate editor coordinating the review of this manuscript and approving it for publication was Zheng H. Zhu.

Industries are still reliant on classical control theory for high-risk aerospace applications such as LV attitude control, inasmuch as these techniques, usually leading to the implementation of proportional-integral-derivative (PID) controllers [1], [2], are deeply understood and validated, and offer reliable procedures for design, analysis, and verification. However, a review of historical LV data from 1990 to 2002 revealed that 41% of failures might have been mitigated by advanced GN&C technologies [3]. Moreover, even though classical control methods are typically able to meet basic flight requirements, the next generation of LVs calls for improved system performance, additional robustness to recover from severe off-nominal conditions, and a reduction of the effort associated with the development of high-fidelity models to be used for running extensive campaigns of simulation tests.

It is apparent that these objectives may only be met by advanced, cost-effective control design techniques and, in this respect, adaptive control has been investigated as a means to adjust the control algorithm to unpredictable, yet somehow sensed, changes in the system response. More precisely, Model Reference Adaptive Control (MRAC) [4] has been proposed in order to manage systems with uncertain parameters, and to maintain stability also in the presence of

unmodeled dynamics. MRAC adapts the control law so as to minimize the difference between output of the controlled system and response of a reference model. Since MRAC design leads to control laws that are inherently nonlinear [5], their behaviour is not always predictable, which is a serious concern from an industrial point of view.

Adaptive Augmenting Control (AAC) has been introduced for the Space Launch System (SLS) [6] as a way to retain the architecture of classically designed linear control systems (baseline controllers, BC, in what follows), while consistently and predictably improving performance and robustness, particularly in off-nominal conditions [7], [8]. This is obtained by introducing a multiplicative forward adaptive law, whose primary principle of operation is to increase the system gain in order to minimize the error with respect to a reference model, while a gain reduction capability is related to the frequency response characteristics of the closed-loop system. Even though, in facts, in nominal conditions the LV fully relies on BC functionalities, a sound and suitable demonstration of AAC stability characteristics in scattered, off-nominal, conditions is not yet available [7], [9], and a significant effort is required to validate the design. This is realized through the evaluation of phase and gain margins in a number of design points along the trajectory, as well as by extensive simulation campaigns using a high-fidelity model of the vehicle in a variety of scattering and external disturbances scenarios, including vehicle failures [10].

In spite of the aforementioned developments in the area of LV control law adaptation, interest in robust multi-variable design techniques is still ongoing, and the $\mathcal{H}_\infty$ [11] methodology deserves attention for replacing the classical PID-type approach to attitude control with more sophisticated and performing solutions. $\mathcal{H}_\infty$ technique aims at finding a control law that minimizes the $\mathcal{H}_\infty$ norm of a suitably defined closed-loop transfer function. Weighting functions are specified in order to express stability and performance requirements (e.g., steady-state error, controller bandwidth, and time response), even though it is not always clear how to define a specific requirement in terms of a single or multiple weights.

In order to deal with rapidly changing dynamics, gain-scheduling is commonly adopted [12], that is, several controllers are designed at various operating points, scheduled over time or other meaningful variables (such as the so called non-gravitational velocity), in the same fashion as in more traditional control methods. However, gain-scheduling does not provide any formal stability or performance proof for fast variations of the scheduling variable, and its effectiveness is justified on empirical basis at most. In this respect, the Linear-Parameter-Varying (LPV) technique [13] has been proposed for the synthesis of a scheduled multivariable controller for flexible LV [14], as the resulting control law comes by-design with known stability and performance bounds, provided that it has access to a measure of the time-varying parameters.

It is to be remarked that traditional $\mathcal{H}_\infty$ and LPV techniques may be impractical in real-case scenarios, because they return high-order controllers, with no defined structure and fast dynamics, making their implementation into flight hardware rather difficult. In this respect, the structured $\mathcal{H}_\infty$ design framework appears especially promising, because it allows for tuning fixed-structure (possibly multi-loop) linear controllers using the $\mathcal{H}_\infty$ methodology [15].

The feasibility of structured $\mathcal{H}_\infty$ design approach for the control of a flexible LV during the ascent phase has been investigated in recent papers [16], [17], that take advantage of the availability of commercial software codes allowing for a streamlined solution of the $\mathcal{H}_\infty$ optimization problems in standard form. Nevertheless, in practical scenarios, structured $\mathcal{H}_\infty$ control still requires a significant effort and a thoughtful iterative design process, that heavily rely on the designer experience, in order to properly shape the weighting functions so that requirements on stability and robustness performance are met.

To address these issues, an automated structured $\mathcal{H}_\infty$ tuning scheme based on GA is presented in this paper for the attitude control of a LV in atmospheric flight. The resulting control law guarantees performance and satisfies a set of robustness/stability specifications typical of industrial practice, while relieving the designer from the necessity of a substantially trial-and-error tuning (or re-tuning) process. Control design process is carried out by parameterizing the weighting functions, and setting up a two-layer max-min global optimization problem. The obtained solution will meet a given set of requirements formulated in frequency or time domain. Typical specifications include, but are not limited to, bounded stability margins, attitude tracking capabilities, wind-gust disturbance rejection, aerodynamic load relief, and control actuation reduction. The proposed hybrid optimization approach combines (i) a GA for the solution of the outer problem that involves the definition of the weighting function parameters, and (ii) a structured $\mathcal{H}_\infty$ synthesis that leads to the definition of control law gains at the inner level.

Use of GAs for control system design in aerospace system has been widely investigated and discussed, since the pioneering work of Goldberg [18]. GA is a population-based meta-heuristic algorithm for global optimization inspired by natural evolution, that has been successfully applied to a wide range of real-world problems of significant complexity. In particular, it is well-suited for multi-modal and non-convex problems, as its stochastic nature provides greater chances to evade from local optima than greedy methods. In most cases, GA is used to directly tune a fixed-structure control system and, among a number of applications, a systematic design procedure named GA-based PID tuning is proposed in [19], where GA is tasked with selecting the PID gains so as to minimize a weighted combination of objective functions that includes integral square error, integral absolute error, and integrated time absolute error. Among many applications this approach has proved effective for tuning the longitudinal control loop of a fixed wing aircraft [20], for the attitude stabilization of a quad-rotor [21], and for

the synthesis of a robust servomechanism linear quadratic regulator on a fixed-wing UAV [22]. A GA-based tuning, where a robust design optimization (RDO) problem [23] is solved, has been recently presented for improving the performance of an adaptive architecture for the attitude control of LVs [24].

In this study the problem of controlling a LV in atmospheric flight is stated, and a linear time-varying model, representative of a medium-size LV [2] is recalled, that features the degrees of freedom of planar motion and the first bending mode superimposed as small vibrations about the rigid-body states. A set of stability and performance requirements, currently adopted in LV attitude control, is specified, together with a baseline flight control system developed according to classical guidelines for LVs, that guarantees stability while leaving room for substantial improvements in terms of robust stability and performance.

First, the design problem is formulated as a structured $\mathcal{H}_\infty$ control problem in standard form, and the weighting functions are defined so as to enforce the requirements. This leads to the synthesis of a gain-scheduled manually-tuned structured $\mathcal{H}_\infty$ controller with two operating modes, that is, drift-reduction and load-relief, which are enforced at different phases of flight in order to effectively deal with the variation of system parameters and, to some extent, design objectives along the vehicle ascent trajectory [25].

Next, a global constrained max-min optimization problem is posed and solved by GA and structured $\mathcal{H}_\infty$, where requirements are explicitly taken into consideration. The resulting procedure is fully automated and allows to devise the controller, referenced as GA-$\mathcal{H}_\infty$, at an arbitrary number of operating points. A second hybrid optimization procedure is also proposed in order to design a controller, dubbed GA-$\mathcal{H}_\infty^{\mathcal{A}}$, obtained by exploiting the GA in combination with an augmented structured $\mathcal{H}_\infty$ control synthesis technique, where the parametric structure of the model uncertainties is directly taken into account in the $\mathcal{H}_\infty$ problem formulation, so as to improve robustness. To this end, an LFT model of the flexible LV with uncertainty on rigid-body parameters and bending mode characteristics (i.e., frequency) is devised.

Performances of the novel, optimally tuned controllers GA-$\mathcal{H}_\infty$ and GA-$\mathcal{H}_\infty^{\mathcal{A}}$ are assessed though μ-analysis [26] and by means of Monte Carlo simulation campaigns in the time domain, with scattered uncertainty parameters and stochastic wind gust disturbances.

The paper is organized as follows. In Section 2 the LV model with uncertainty is presented, and the mathematical form of wind disturbances is recalled. Control system requirements are recalled in Section 3, where the BC is also described. Section 4 deals with the design of the structured $\mathcal{H}_\infty$ controller, while developments of GA-$\mathcal{H}_\infty$ and GA-$\mathcal{H}_\infty^{\mathcal{A}}$ are illustrated in Section 5. The different control laws are analyzed and discussed in Section 6, and a section of Conclusions ends the paper.

II. FORMULATION

A. VEHICLE DYNAMICS

A time-varying linear model of an axisymmetric LV configuration where the couplings between pitch and yaw motions are ruled out is considered. Main features are as follows: i) rigid-body translational and rotational dynamics, ii) rocket flexibility in terms of first bending mode, iii) aerodynamic and propulsive forces and moments, and iv) TVC actuators dynamics. The model provides a good trade-off between simplicity and accuracy, as it considers all LV dynamics relevant for attitude control design while allowing for the application of classical stability analysis methods in the frequency domain, as for instance gain and phase margin evaluation and verification with respect to requirements currently adopted for flight certification.

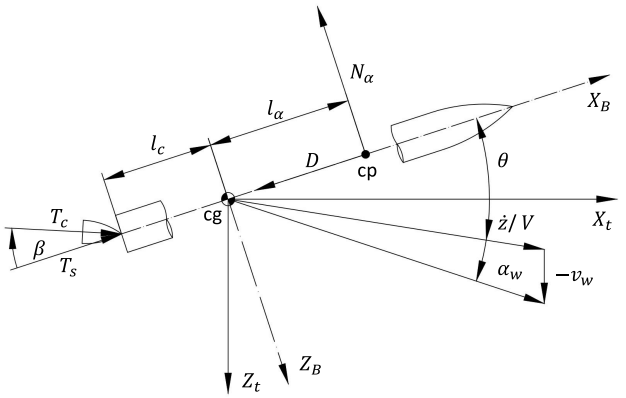

FIGURE 1. Sketch of the LV model.

Rotational (about pith axis) and lateral drift motions of the body frame $\mathcal{B}$ are described with respect to a non-stationary frame $\mathcal{T}$ tangent to the nominal ascent trajectory, as shown in Fig. 1. Accordingly, the governing equations are

$$\ddot{z} = a_1 V\left(\theta + \frac{\dot{z}}{V} - \alpha_w\right) + a_4\theta + a_3\beta \tag{1}$$

$$\ddot{\theta} = A_6\left(\theta + \frac{\dot{z}}{V} - \alpha_w\right) + K_1\beta \tag{2}$$

$$\alpha = \theta + \frac{\dot{z}}{V} - \alpha_w \tag{3}$$

with high-level coefficients

$$A_6 = \frac{N_\alpha l_\alpha}{I_{yy}} \quad K_1 = \frac{T_c l_c}{I_{yy}} \quad a_1 = -\frac{N_\alpha}{mV}$$
$$a_3 = \frac{T_c}{m} \quad a_4 = -\frac{(T_t - D)}{m}$$

where z and $\dot{z}$ are drift and drift rate of the center of mass (cg) along the normal axis of the trajectory frame, respectively, and θ is the pitch angle. Next, m and I_{yy} are LV mass and moment of inertia, l_α and l_c are aerodynamic and control moment arms, $T_t = T_s + T_c$ the total thrust force composed of the sustained thrust T_s and the control (swivelled) thrust T_c, β is the nozzle angle, N_α the aerodynamic normal force

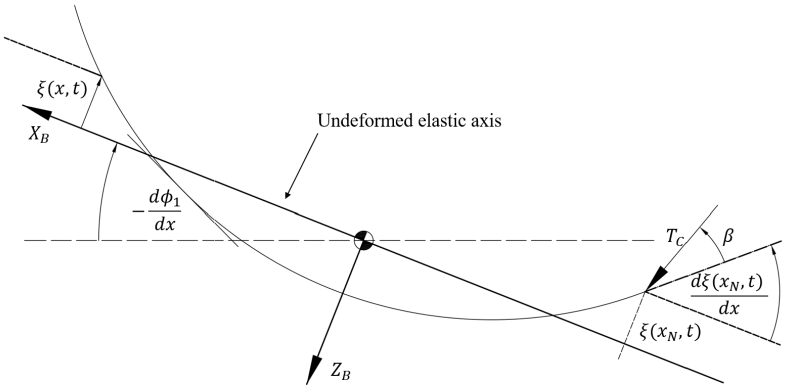

FIGURE 2. Flexible vehicle configuration.

applied in the center of pressure (cp), and D the aerodynamic axial force. Also, α is the angle of attack, V the velocity of the LV, $\alpha_w = v_w/V$ is the wind-induced angle of attack, and v_w is the wind velocity.

The elastic degrees of freedom are taken into consideration by means of the modal decomposition method [27], and relevant variables are recalled in Fig. 2, where a sketch of the deformed shape of the LV is reported.

Let $\xi(x, t)$ be the elastic deflection, and x_N the longitudinal coordinate of the nozzle hinge. The displacement at a distance x along the vehicle in body frame is given by

$$\xi(x,t) = \sum_{i=1}^{N} \phi_i(x) q_i(t) \tag{4}$$

where x is the abscissa along the LV longitudinal axis, N is the number of modes, ϕ_i is i^{th} mode shape in the pitch plane, normalized over mass, and q_i is the generalized coordinate of i^{th} mode. The motion of each bending mode (BM) is described by

$$\ddot{q}_i + 2\zeta_i\omega_i\dot{q}_i + \omega_i^2 q_i = -T_c\phi_i\beta \tag{5}$$

where ω_i and ζ_i are natural frequency and damping ratio of i^{th} BM, respectively. Only the first BM is here considered because it appears at relatively low frequency with respect to the control system bandwidth, whereas higher-order modes have minor effects on system stability.

Vehicle model is completed by the output equations at the inertial navigation system (INS) location x_{INS}, where the contribution of flexible mode is summed to that of rigid motion. They read

$$\theta_{INS} = \theta + \sigma_1(x_{INS})q \tag{6}$$
$$\dot{\theta}_{INS} = \dot{\theta} + \sigma_1(x_{INS})\dot{q} \tag{7}$$
$$z_{INS} = z - \phi_1(x_{INS})q \tag{8}$$
$$\dot{z}_{INS} = \dot{z} - \phi_1(x_{INS})\dot{q} \tag{9}$$

An open source implementation of the mathematical model of the vehicle is available on GitHub.[1]

B. TVC ACTUATOR DYNAMICS

The actuator model features two serially connected transfer functions, representing a second-order dynamics plus a pure time delay, τ, modelled through a second order Padé approximation, as

$$\begin{bmatrix}\dot{d}\\ \ddot{d}\end{bmatrix} = \begin{bmatrix}0 & 1\\ -\frac{12}{\tau^2} & -\frac{6}{\tau}\end{bmatrix}\begin{bmatrix}d\\ \dot{d}\end{bmatrix} + \begin{bmatrix}0\\ -\frac{12}{\tau^2}\end{bmatrix}\beta_c \tag{10}$$

with

$$\beta_{\hat{c}} = \dot{d} + \beta_c \tag{11}$$

where β_c and $\beta_{\hat{c}}$ are, respectively, actual and delayed TVC commands. The transfer function of the TVC dynamics is

$$W_{TVC}(s) = \frac{\beta}{\beta_{\hat{c}}} = \frac{\omega_{TVC}^2}{s^2 + 2\zeta_{TVC}\omega_{TVC}\, s + \omega_{TVC}^2} \tag{12}$$

where ζ_{TVC} and ω_{TVC} are damping ratio and natural frequency, respectively.

C. UNCERTAINTY MODEL

An augmented, structured uncertainty model of LV, to be used for the GA-$\mathcal{H}_\infty^{\mathcal{A}}$ synthesis, is derived based on linear fractional transformation (LFT). Let $p = p_{nom}(1 + p_r\delta)$ be an arbitrary uncertain parameter, where p_{nom} is its nominal value, p_r is the maximum scattering, and $\delta \in [0, 1]$ the normalized range of variation. This multiplicative uncertainty representation corresponds to the upper LFT function

$$F_u(M, \Delta_u) = \left(\begin{bmatrix}0 & 1\\ p_{nom}p_r & p_{nom}\end{bmatrix}, \delta\right) \tag{13}$$

By repeatedly applying the above transformation to all uncertain parameters, and recalling the fundamental property of LFT that the interconnection of LFTs is still an LFT, a

[1] https://github.com/AlessandroZavoli/Rocket-Attitude-Dynamics

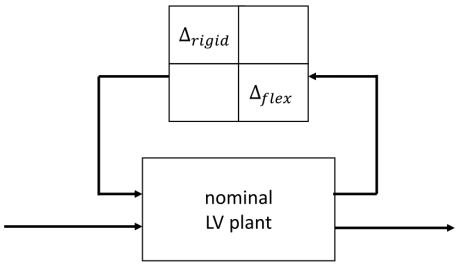

FIGURE 3. LFT structured uncertainty LV model.

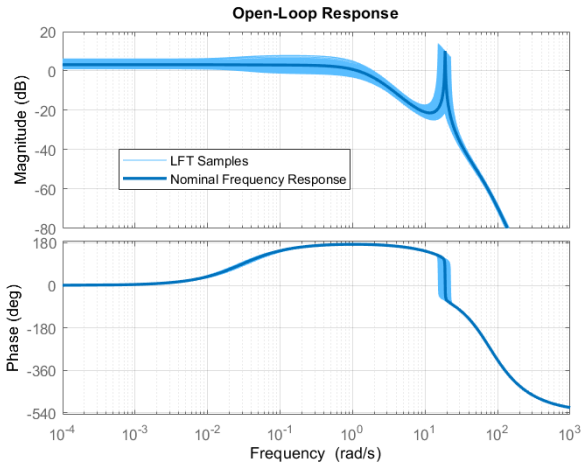

FIGURE 4. LFT frequency response of pitch channel at $t = 72$ s.

LFT model of the LV in the $P - \Delta$ form is devised (see Fig. 3), where P corresponds to the nominal model and Δ is a perturbation matrix, with diagonal structure and (possibly repeated) entries δ_i corresponding to the normalized variation of the i-th parameter. Assuming that uncertainty directly affects the so-called high-level rigid-body (A_6, K_1, a_1, a_3, a_4, and ω_{TVC}) and modal (ω_{BM}) parameters, we define $\Delta = \text{diag}\left(\Delta_{LV_{\text{rigid}}}, \Delta_{LV_{\text{flex}}}\right)$, being

$$\Delta_{LV_{\text{rigid}}} = \left\{\text{diag}\left(\delta_{A_6}, \delta_{K_1}, \delta_{a_1}, \delta_{a_3}, \delta_{a_4}, \delta_{\omega_{TVC}} I_6\right),\ \|\delta_i\|_\infty \le 1\right\} \quad (14)$$

$$\Delta_{LV_{\text{flex}}} = \left\{\delta_{\omega_{BM}} I_2,\ \|\delta_i\|_\infty \le 1\right\} \quad (15)$$

where I_2 and I_6 are unit matrices of rank 2 and 6, respectively.

The generation of the LFT model is streamlined once the state-space model is available, as the MathWorks's Robust Control Toolbox [28] greatly reduces the development effort. Note that, due to augmentation, the system order of the LFT model increases to 22 with respect to the 14 states of the nominal LV model.

The open-loop transfer function $T_{\beta \to \theta_{ins}}$ for the LV uncertain model evaluated at $t = 72$ s, when dynamic pressure is maximum (Q-max), is shown in Fig. 4. Two regions are apparent where the effects of uncertainty are more significant, that is, the dispersion of the Bode plot is larger. The first one is related to rigid-body parameter variations (on the left), and the second one to bending mode scattering (on the right). Nominal values of high-level parameters and their range of uncertainty at the above flight time are reported in Table 1.

TABLE 1. High-level parameters and uncertainty ranges at max-Q condition.

Parameter	Nominal value	Scattering (%)
A_6	3.27	±30
K_1	4.54	±30
ω_{BM}	18.9 rad	±20
a_1	-0.0154	±5
a_3	20.4017	±5
a_4	-27.0598	±5
ω_{TVC}	70 rad	±5

D. WIND MODEL

The wind disturbance model, considered for flight control system (FCS) analysis and validation, is formulated according to the NASA guidelines [29], where the normal wind velocity component v_w is expressed by coloring a white noise n_w through a Dryden filter $G_w = \frac{v_w(s,h)}{n_w(s)}$ with transfer function

$$G_w(s,h) = \frac{\sqrt{\frac{2}{\pi}\frac{V(h) - v_{wp}(h)}{L(h)}}\sigma^2(h)}{s + \frac{V(h) - v_{wp}(h)}{L(h)}} \quad (16)$$

being $L(h)$ and $\sigma(h)$ the turbulence length scale and standard deviation versus altitude h, respectively. Their values are given in tabular form in [29] for three levels of turbulence (low, medium, and high). The altitude-dependent steady-state wind velocity profile $v_{wp}(h)$ is defined as

$$v_{wp}(h) = \begin{cases} 10A\left[\left(\frac{h}{H_l}\right)^{0.9} - 0.9\frac{h}{H_l}\right] & \text{for } 0 \le h < H_l \\ A & \text{for } H_l \le h \le H_f - H_u \\ \frac{A}{2}\left[1 - \cos\left(\frac{\pi}{H_u}\left(h - H_f\right)\right)\right] & \text{for } H_f - H_u < h \le H_f \end{cases} \quad (17)$$

with gust amplitude $A = 14$ m/s, leading-edge altitude $H_l = 2.000$ m, trailing-edge altitude $H_u = 2.500$ m, and terminal altitude $H_f = 25.000$ m

Figure 5 shows the velocity v_{wp} (steady-state profile), and a few random samples of the stochastic gust (gray lines). One sample (blue line) is highlighted for the sake of clarity, and will be referenced as nominal wind profile in the discussion of results.

III. BASELINE CONTROLLER

A. CONTROL SYSTEM REQUIREMENTS

Table 2 reports the set of specifications for LV attitude control loops, expressed in terms of stability margins, where: i) Aero gain margin (GM), Rigid GM, and Rigid phase margin (PM), associated to the rigid-body dynamics, are the low-frequency

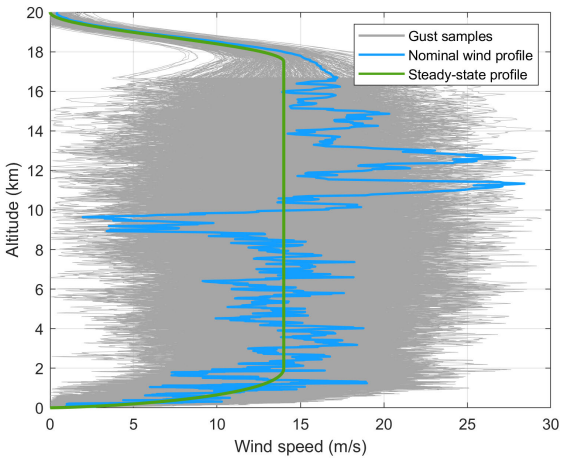

FIGURE 5. Wind velocities vs. altitude.

margins (for the present model the highest rigid-body frequency is below 8.4 rad/s at Q-max), and ii) Flex GM and Flex PM, related to the first bending mode (BM), represent the group of high-frequency margins (frequency above 8.4 rad/s at Q-max). The phase margin (PM) requirement is commonly formulated in term of delay margin, and expressed in units of time.

TABLE 2. Stability requirements.

Rigid-body margins			Elastic mode margins	
Aero GM	Rigid PM	Rigid GM	Flex GM	Flex PM
≥ 6 dB	≥ 100 ms	≤ -6 dB	≤ -3 dB	≥ 50 ms

Table 3 shows the performance requirements, that are to be satisfied in different phases of flight. To this end, two control modes, namely load-relief and drift-minimum are considered [25]. Load-relief mode is used at high values of dynamic pressure, that is, in the time interval $50 \leq t \leq 90$ s, when wind gusts may produce large values of angle of attack, and the resulting structural loads are to be maintained within the specified $Q\alpha$ safety envelope. Since the reduction of $Q\alpha$ is obtained at the expense of larger offsets from the nominal trajectory, the drift-minimum control mode is adopted in the other phases of flight in order to achieve good tracking performance, that is, to minimize lateral drift and drift-rate while keeping low the aerodynamic load.

TABLE 3. Performance requirements.

Requirement	Metric	Bound
Aerodynamic load	$Q\alpha$	$< Q\alpha$ safety envelope
Lateral drift	Z_{max}	< 500 m
Lateral rate drift	$\dot{Z}_{max}$	< 15 m/s
TVC angle deflection	β_{max}	< 6 deg

BC architecture features two PD elements for attitude and lateral dynamics, plus a second-order low-pass filter H_{LP} and a notch filter H_N to phase-stabilize and attenuate the BM, so that the control law is, in the frequency domain

$$\boldsymbol{K}_{BC}(s) = [K_{P_\theta} \quad K_{D_\theta} \quad K_{P_z} \quad K_{D_z}] H_N(s) H_{LP}(s) \tag{18}$$

where K_{P_θ}, K_{D_θ} and K_{PZ}, K_{DZ} are gain coefficients for the attitude and drift control loops, respectively.

An appropriate selection of gains K_{P_θ} and $K_{D_{\dot\theta}}$ is obtained by enforcing the stability requirements in Table 2 into the simplified system obtained by neglecting lateral, TVC and bending mode dynamics [12], that is

$$\ddot{\theta} = A_6\theta + K_1\beta \tag{19}$$

with $\beta = K_P\theta + K_D\dot{\theta}$. In this situation, the open-loop transfer function of the controlled system is

$$GK(s) = \frac{K_1(K_{D_\theta}s + K_{P_\theta})}{s^2 - A_6} \tag{20}$$

with

$$K_{P_\theta} = \frac{2A_6}{K_1} \quad K_{D_\theta} = \frac{\sqrt{A_6}}{K_1} \tag{21}$$

Gains for lateral, z-axis control are as small as one or two orders of magnitude lower than K_{P_θ} or K_{D_θ} in order to satisfy the constraints on maximum drift and drift-rate in Table 3 without hindering the attitude error performance [24].

Low-pass and notch filter coefficients are set according to the guidelines provided by Wie [30]. In particular, a cascade of three second-order notch filters is adopted for BM attenuation, as

$$\begin{aligned} H_N(s) = & \frac{s^2 + 2\zeta_{N_1}\underline{\omega}_{BM}s + \underline{\omega}_{BM}^2}{s^2 + 2\zeta_{D_1}\underline{\omega}_{BM}s + \underline{\omega}_{BM}^2} \\ & \cdot \frac{s^2 + 2\zeta_{N_2}\omega_{BM}s + \omega_{BM}^2}{s^2 + 2\zeta_{D_2}\omega_{BM}s + \omega_{BM}^2} \\ & \cdot \frac{s^2 + 2\zeta_{N_3}\overline{\omega}_{BM}s + \overline{\omega}_{BM}^2}{s^2 + 2\zeta_{D_3}\overline{\omega}_{BM}s + \overline{\omega}_{BM}^2} \end{aligned} \tag{22}$$

where $\underline{\omega}_{BM} = 0.9\,\omega_{BM}$ and $\overline{\omega}_{BM} = 1.1\,\omega_{BM}$, being ω_{BM} the (nominal) bending mode frequency. The damping coefficients ζ_{N_i} and ζ_{D_i}, with $\zeta_{N_i} < \zeta_{D_i}$, specify bandwidth and peak level of filter attenuation, respectively. We set $\zeta_{N_2} = 0.06$ and $\zeta_{D_2} = 0.3$ for the center filter, and $\zeta_{N_1} = \zeta_{N_3} = 0.02$ and $\zeta_{D_1} = \zeta_{D_3} = 0.1$ for the left and right filters, respectively.

The non-minimum phase filter H_{LP} is implemented in order to further phase-stabilize the BM, that is, to move the phase of elastic dynamics near 0 deg. The transfer function reads

$$H_{LP}(s) = \frac{s^2 + 2\zeta_z\omega_z s + \omega_z^2}{s^2 + 2\zeta_p\omega_p s + \omega_p^2} \tag{23}$$

where pole and zero locations are specified so that they share the same natural frequency (close to ω_{BM}), with $\zeta_p > \zeta_z$. The values $\zeta_p = 0.32$ and $\zeta_z = 0.1$ have been selected for the present application.

Gains and filter parameters are scheduled versus time over a grid of 15 points, evenly spaced by 10 s, and linearly interpolated throughout the flight. Note that the same design points are used for all controllers.

IV. STRUCTURED $\mathcal{H}_\infty$ CONTROL

Consider a linear time-invariant plant P, and a dynamic controller $K(\boldsymbol{\Theta}) \in \mathcal{K}$, that is, a controller with a given structure $\mathcal{K}$, in the form of Eq. (18), and tunable parameters $\boldsymbol{\Theta} \in \mathbb{R}^d$. The structured $\mathcal{H}_\infty$ optimization problem is stated as [31]

$$\begin{aligned} &\underset{\Theta}{\text{minimize}} \in \mathbb{R}^d \boldsymbol{\Theta} \in \mathbb{R}^d \gamma = \|\boldsymbol{T}_{w\to z}(P,\ K(\boldsymbol{\Theta}))\|_\infty \\ &\text{subject to } K(\boldsymbol{\Theta}) \in \mathcal{K} \quad \text{closed-loop stabilizing} \end{aligned} \tag{24}$$

where $\boldsymbol{T}_{w\to z}$ is the closed-loop transfer function from the vector of exogenous variables $\boldsymbol{w}$, that includes disturbances and commands, to the regulated output vector $\boldsymbol{z}$. Figure 6 shows the standard $\mathcal{H}_\infty$ problem formulation, where the closed-loop interconnection between system and controller is represented by a lower LFT, that is, $\boldsymbol{T}_{w\to z} = F_l(P, K)$ [32], and u and v represent, respectively, control input and feedback to the controller. The input ($\boldsymbol{W}^{\text{in}}$) and output ($\boldsymbol{W}^{\text{out}}$) weighting matrices, also reported in the figure, provide means to specify stability and performance requirements in term of $\boldsymbol{T}_{w\to z}$, as well as a practical way to scale input and output signals in order to obtain (as much as possible) a normalized problem where $\|\boldsymbol{w}\|_\infty \leq 1$ and $\|\boldsymbol{z}\|_\infty \leq 1$.

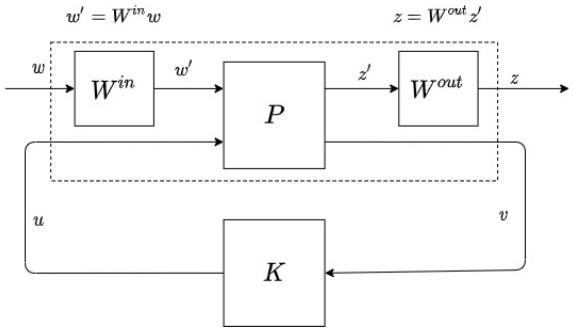

FIGURE 6. Standard $\mathcal{H}_\infty$ interconnection with explicit weighing functions.

Figure 7, where P corresponds to the LV model, shows the block diagram of the $\mathcal{H}_\infty$ architecture. The exogenous input vector $\boldsymbol{w}$ includes the reference variable vector $\boldsymbol{r}$, with components given by lateral drift Z_{ref} and drift rate $\dot{Z}_{ref}$, attitude θ_{ref}, and attitude rate $\dot{\theta}_{ref}$, together with the wind disturbance α_w, that is

$$\boldsymbol{w} = [Z_{ref}\ \dot{Z}_{ref}\ \theta_{ref}\ \dot{\theta}_{ref}\ \alpha_w]^T \tag{25}$$

The elements of the regulated output vector $\boldsymbol{z}$, written as

$$\boldsymbol{z} = [Z_{ins}\ \dot{Z}_{ins}\ \theta_{ins}\ \dot{\theta}_{ins}\ \theta_e\ \beta\ Q\alpha]^T \tag{26}$$

are the measurements Z_{ins}, $\dot{Z}_{ins}$, θ_{ins}, $\dot{\theta}_{ins}$, the attitude error signal e_θ, and the performance metrics β and $Q\alpha$, related to actuation effort and aerodynamic bending load, respectively.

Finally, the weighting functions on input/output channels are defined as

$$\boldsymbol{W}^{\text{in}} = diag\left(W_{Z_{ref}},\ W_{\dot{Z}_{ref}},\ W_{\theta_{ref}},\ W_{\dot{\theta}_{ref}},\ W_{\alpha_w}\right) \tag{27}$$

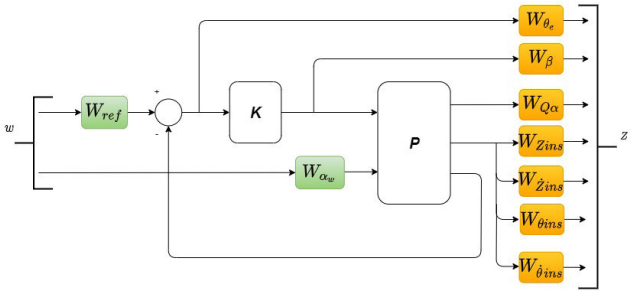

FIGURE 7. Structured $\mathcal{H}_\infty$ interconnection for LV attitude control.

$$\begin{aligned} \boldsymbol{W}^{\text{out}} = diag\Big(&W_{Z_{ins}},\ W_{\dot{Z}_{ins}},\ W_{\theta_{ins}},\\ &W_{\dot{\theta}_{ins}},\ W_{\theta_e},\ W_\beta,\ W_{Q\alpha}\Big) \end{aligned} \tag{28}$$

Solution of the problem in Eq. (24) is not a trivial task, due to its non-convexity and the possible convergence to a local minimum. Nevertheless, the adopted solver is rather efficient and, by using a combination of local optimization methods and a simple restart strategy, provides suitable solutions in reasonable computational time for a number of test cases [33].

Specific guidelines on the selection of input/output weighting functions are briefly recalled heretofore, with reference to [25], [34] where a detailed analysis on the application of the structured $\mathcal{H}_\infty$ design to the VEGA launcher is discussed. Note that only constant (in the form $W(s) = C$ or $W(s) = 1/D$, being D an assigned coefficient) or first-order weighting functions are considered, as the use of higher-order weights is found to provide minimal improvements at the cost of increased complexity.

Output weights are used to limit the frequency content of error or output signals in vector $\boldsymbol{z}$ (see Fig. 7). The weights W_{Zref} and $W_{\dot{Z}ref}$, related to the regulated drift and drift-rate output variables (Z_{ref} and $\dot{Z}_{ref}$), are expressed in terms of the requirements in Table 3, as

$$W_{Zref} = Z_{max}^{-1} \quad W_{\dot{Z}ref} = \dot{Z}_{max}^{-1} \tag{29}$$

Analogously, the weight on $Q\alpha$ output should have the same form, as function of the maximum aerodynamic load. By introducing a parameter D_α, and leveraging on the fact that the values of dynamic pressure Q at the design points are known (from the nominal trajectory), this weight is written as

$$W_{Q\alpha} = \frac{1}{QD_\alpha} \tag{30}$$

The weighting functions W_{θ_e} and $W_{\theta ins}$, associated to the output signals θ_e and θ_{ins}, are specified in terms of Aero-GM and Rigid-GM so as to guarantee that the requirements on stability and tracking performance are met. In particular, $W_{\theta_e}^{-1}(s)$ is a first-order high-pass filter used to limit the sensitivity function of the closed loop system $\boldsymbol{S}_\theta(s)$, given by

$$W_{\theta_e} = \left(\frac{s/M + \omega}{s + \omega A}\right)^{-1} \tag{31}$$

Since $W_{\theta_e}^{-1}(s)$ plays the role of a sensitivity weight, A is to be small enough to enforce good low-frequency disturbance rejection characteristics, ω selects the control bandwidth, to be specified according to the LV model, and M is expressed so as to obtain (approximately) the desired stability margins GM and PM, according to

$$\text{GM} \geq \frac{M}{M-1} \quad \text{PM} \geq 2\arcsin\left(\frac{1}{2M}\right) \geq \frac{1}{M}[\text{rad}] \tag{32}$$

For instance, for $M = 2$ one has GM = 6 dB and PM $\approx$ 29 deg.

Conversely, $W_{\theta_{ins}}^{-1}(s)$ is a first-order low-pass filter that limits the complementary sensitivity function $\boldsymbol{T}_\theta(s)$, given by

$$W_{\theta_{ins}} = \left(\frac{s+\omega A}{s/M+\omega}\right)^{-1} \tag{33}$$

where A is equal to the high-frequency asymptote of $W_{e_\theta}^{-1}(s)$ in order to satisfy the classical constraint $\boldsymbol{S} + \boldsymbol{T} = \boldsymbol{I}$. The value of ω must be lower than the bending mode frequency so as to limit coupling with flexible dynamics, yet sufficiently high for improving attitude tracking performance, whereas M is to be small for adequate noise rejection.

Next, a constant weighting function $W_{\dot\theta} = 1/\dot\theta_{max}$ is selected for the angular rate signal $\dot\theta_{ins}$. The value $\dot\theta_{max}$ is specified as the largest pitch rate observed in preliminary simulation runs where the BC was used. Finally, the weight W_β, that takes into account the frequency content of β as resulting from the $H_N(s)$ and $H_{LP}(s)$ filters in the control loop [25], reads

$$W_\beta(s) = \frac{C_\beta}{H_N(s)H_{LP}(s)} \tag{34}$$

Input weighting functions allow for the description of the expected or known frequency content of exogenous signals $\boldsymbol{w}$. However, this information is often not available in practice, and the weights are mainly the result of a manual and iterative design process aimed at providing a suitable balance between input and output channels [35]. Static weights are here considered, with the relevant exception of W_{α_w}, where the input behaves as a colored noise with transfer function $G_w(s)$ (Eqs. (16)–(17)), and we have $W_{\alpha_w}(s) = C_{\alpha_w}G_w(s)$.

Note that W_{Zr} and $W_{\dot Zr}$ are specified so as to balance drift and drift rate channels, respectively, $W_{r_{\dot\theta}}$ acts on both pitch and pitch rate channels, and W_{r_θ} is set to limit the maximum pitch angle to 1 deg.

Table 4 reports the values of the weight parameters for the drift-reduction and load-relief modes. One set of constant parameters is specified for each mode so as to simplify tuning of the gain-scheduled controller.

TABLE 4. Weighting function coefficients for the structured $\mathcal{H}_\infty$ control synthesis. Data in round brackets are for drift-reduction mode.

Weight Parameters		Value		Units
W_{θ_e}	A	0.03		rad
	M	1.95		rad
	ω	6.50		rad/s
$W_{\theta_{ins}}$	A	1.95		rad
	M	0.01		rad
	ω	15.00		rad/s
$W_{\dot\theta_{ins}}$	D	0.232		rad/s
$W_{Z_{ins}}$	D	1,500.00	(500.00)	m
$W_{\dot Z_{ins}}$	D	13.00	(15.00)	m/s
W_β	D	5.73		deg
$W_{Q\alpha}$	D	2.50	(4.50)	deg
$W_{Z_{ref}}$	C	22.00	(15.00)	m
$W_{\dot Z_{ref}}$	C	22.00	(15.00)	m/s
$W_{\dot\theta_{ref}}$	C	3.15		deg/s
$W_{\theta_{ref}}$	C	1.00		deg
W_{α_w}	C	0.01		rad

V. HYBRID GA-$\mathcal{H}_\infty$ CONTROLLERS

In order to improve the controller design process and automate the procedure for defining the weighting functions, a nested optimization approach is adopted, where the coefficients of $\boldsymbol{W}^{\text{in}}$, $\boldsymbol{W}^{\text{out}}$ and K are determined. In particular, the solution of the structured $\mathcal{H}_\infty$ problem (inner-level) is carried out by the Matlab solver *structhinf*, and the evaluation of weighing function parameters (outer-level) is managed by GA, so that the controller obtained from the hybrid GA-$\mathcal{H}_\infty$ design provides optimal performance and guarantees the desired stability margins.

A. GENETIC ALGORITHM

The main features of GA algorithm are recalled in this Section, and further details can be found in [36]. First, an initial population, that is, a collection of solutions (often referred as individuals or chromosomes) is randomly generated trying to cover the search space as well as possible. At each iteration (generation), the fitness of each individual in the population is evaluated. Then, a mating population is created by identifying a number of individuals from the current population, according to a selection operator which tries to promote individuals with a good fitness without sacrificing diversity. Typical selection operators are Stochastic Roulette Wheel and Tournament [36], the latter being used in the present application.

Next, pairs of individuals (parents) are randomly chosen from the mating population and combined for producing new solutions (offsprings) according to the simulated binary crossover rule [37]. The underlying idea is that combining good solutions allows in some way to create new, and hopefully better, solutions. The process is repeated until a new population, usually with the same dimension of the previous one, is created.

Eventually, a few randomly-chosen individuals of the offspring population undergo a mutation process, based on the simple albeit effective adaptive Gaussian mutation operator [38], with the aim of increasing the population diversity. This new population replaces the previous one, and this phase is iterated until some termination criterion (e.g., maximum number of generation) is met. As a minor, yet

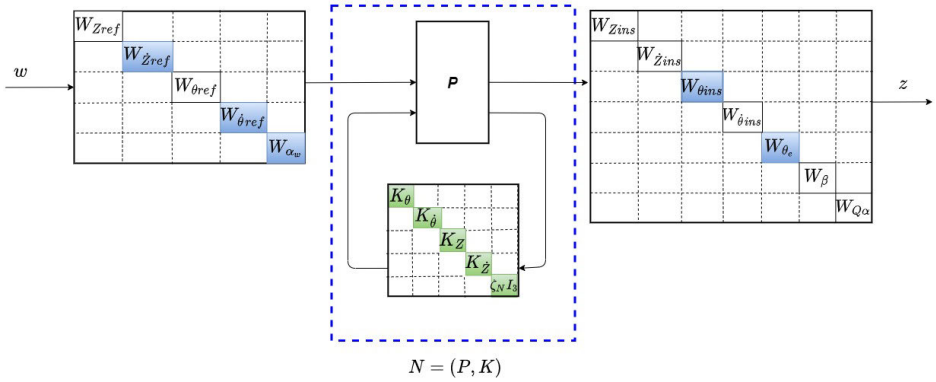

FIGURE 8. Standard form of the hybrid GA-$\mathcal{H}_\infty$ optimization problem.

important tweak, elitism is enforced, that is, at the end of each generation, the N_p^e best individuals of the parent population are copied into the offspring population, thus preserving the best solution from being accidentally lost in the evolution process.

Some control over the population diversity is often needed. The aim is to avoid an excessive uniformity between individuals that would result in a very inefficient use of the crossover operator, hence in a waste of function evaluations. To overcome this problem, an epidemic mechanism is introduced where a diversity metric is defined as the sum over the population of the infinity-norm between any pair of individuals in the search space. If the diversity score falls below a given threshold, a large part of the population dies, that is, it is randomly re-initialized. This mechanism cannot take place more than M^λ times, and not twice within a number N_G^λ of generations.

From a practical point of view, GA performance depends on the choice of selection, mutation and crossover operators, but also on the so-called hyper-parameters, namely, population size (n_P), number of generations (n_G), crossover probability (p_c), and mutation rate (p_m). The latter two parameters represent, respectively, the percentage of parents replaced by offspring, and the probability that an individual will undergo a random mutation.

B. GA-$\mathcal{H}_\infty$ DESIGN

We assume that all weights are fixed-structure functions with tunable parameters $\boldsymbol{x} \in \mathcal{X}$, so that $\boldsymbol{W}^{\text{in}} = \boldsymbol{W}^{\text{in}}(\boldsymbol{x})$ and $\boldsymbol{W}^{\text{out}} = \boldsymbol{W}^{\text{out}}(\boldsymbol{x})$ are proper and stable weighting functions, and $\mathcal{X}$ is a boxed search space. As discussed in Section IV, all weighting functions are restricted to be either static with gain C, or first-order transfer functions in the form of Eq. (31), parametrized by low- and high-frequency asymptotes, A and M, respectively, and crossover frequency ω_b.

Following a preliminary analysis, where the effects of weighting function parameters on controller performance were investigated, the optimization problem is simplified by assuming that only $W_{\dot{Z}ref}$, $W_{\dot{\theta}ref}$, W_{α_w}, W_{θ_e}, and $W_{\theta_{ins}}$ are tunable, whereas the parameters of the remaining functions maintain the values reported in Table 4. Accordingly, the vector of design parameters is

$$\boldsymbol{x} = [C_{\dot{z}_{ref}}\ C_{\dot{\theta}_{ref}}\ C_{\alpha_w}\ M_{\theta_e}\ M_{\theta_{ins}}\ A_{\theta_e}\ A_{\theta_{ins}}\ \omega_{\theta_e}\ \omega_{\theta_{ins}}]^T \quad (35)$$

where the subscripts associate the coefficients to the pertinent weighting functions. The nested GA-$\mathcal{H}_\infty$ optimization problem is posed as

$$\max_{\boldsymbol{x}} J = \max\left(0,\, \gamma(\boldsymbol{\Theta}^\star) - \bar{\gamma}\right) + \sum_j \max\left(0,\, \Sigma_j(\boldsymbol{\Theta}^\star)\right) \quad (36)$$

with

$$\boldsymbol{\Theta}^\star = \arg\min_{\boldsymbol{\Theta}} \left\| \boldsymbol{T}_{w\to z}\left(P\left(\boldsymbol{W}^{\text{in}}(\boldsymbol{x}), \boldsymbol{W}^{\text{out}}(\boldsymbol{x})\right),\, K(\boldsymbol{\Theta})\right)\right\|_\infty$$
$$\text{subject to } K(\boldsymbol{\Theta}) \in \mathcal{K} \text{ closed-loop stabilizing} \quad (37)$$

The functions Σ_j in Eq. (36) are used to express requirements on stability margins (Table 2) so that, when $\Sigma_j < 0$, the i-th specification is satisfied. On the other hand, performance requirements in Table 3 are implicitly satisfied through the $\mathcal{H}_\infty$ optimization when $\gamma < 1$, being the (fixed) weights W_z and $W_{\dot{Z}}$ expressed as in Eq. (29). Finally, by using $\max(0,\ \gamma - \bar{\gamma})$ in the merit index in place of directly minimizing γ, leads to a relaxed problem formulation, where any value of $\gamma < \bar{\gamma}$ is equally valid, thus reducing the computation burden. A value of $\bar{\gamma} = 1.5$ is set according to common practice [31]. The elements of $\boldsymbol{\Theta}$, given by

$$\boldsymbol{\Theta} = \left[K_{P_\theta},\ K_{D_\theta},\ K_{P_Z},\ K_{D_Z},\ \zeta_{N1},\ \zeta_{N2},\ \zeta_{N3}\right]^T \quad (38)$$

are the tunable parameters of the controller K (Eq. (18)), that is, the PD gains on attitude and lateral channels, and the damping coefficients in the numerator of the notch filter transfer function $H_N(s)$, whereas the other parameters of K are set at the same values used in the BC.

Figure 8 shows in blue colour the weighting function parameters directly tuned by GA, and the gains of K determined by the structured $\mathcal{H}_\infty$ synthesis (green). All the other weights (uncoloured) are fixed.

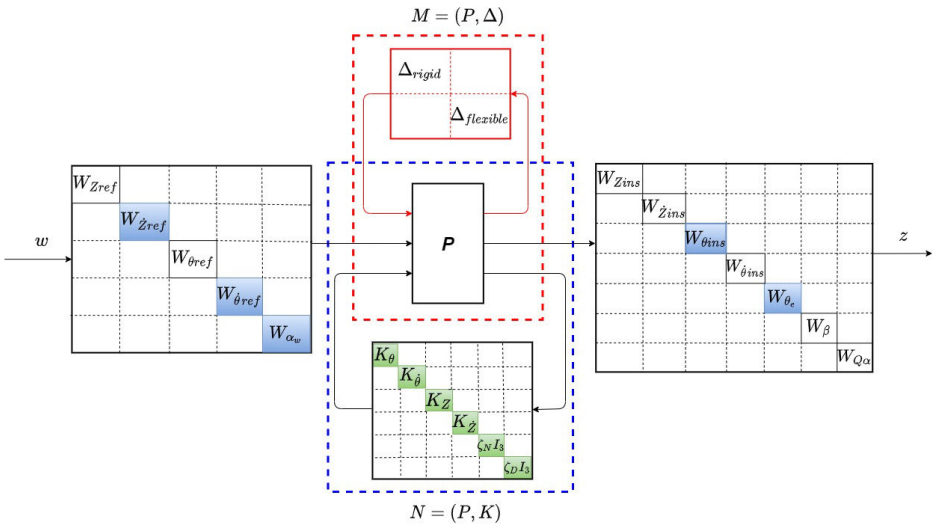

FIGURE 9. Standard form of the augmented structured GA-$\mathcal{H}_\infty^{\mathcal{A}}$ control synthesis problem.

TABLE 5. GA hyper-parameters.

Parameter	Symbol	Value
Selection rule		Tournament (k=2)
Crossover rule		SBX
Mutation rule		Gaussian
Population size	N_P	64
No. of generations	N_G	128
Crossover probability	p_c	0.9
Mutation probability	p_m	0.05
Elite size	N_P^e	128
No. of epidemics	m^λ	5
Epidemics frequency	N_G^λ	128

TABLE 6. Lower and upper bounds of weighting function coefficients for the GA-$\mathcal{H}_\infty$ and GA-$\mathcal{H}_\infty^{\mathcal{A}}$ optimization problems.

Weight parameter	Bounds min	Bounds max	Unit
$C_{\dot{Z}ref}$	15	30	[m/s]
$C_{\dot{\theta}ref}$	0.01	1.5	[deg/s]
C_{α_w}	0.01	4	[deg]
M_{θ_e}	1	3.16	[deg]
$M_{\theta_{ins}}$	1	3.16	[deg]
A_{θ_e}	0	1	[deg]
$A_{\theta_{ins}}$	0	1	[deg]
ω_{θ_e}	0.01	13	[rad/s]
$\omega_{\theta_{ins}}$	13	17.5	[rad/s]

C. GA-$\mathcal{H}_\infty^{\mathcal{A}}$ DESIGN

When the LFT-structured uncertainty LV model is directly considered in the $\mathcal{H}_\infty$ problem formulation [39], a controller that is robustly stable by design to any uncertain configuration in the set Δ of Sec. II-C is developed.

An augmented control synthesis problem is thus posed, the block diagram of which is shown in Fig. 9, where the lower LFT interconnection (in blue) between the model and the controller, and the upper LFT interconnection (in red) for the LV model with high-level uncertain parameters (see again Sec. II-C) are reported. The corresponding optimization problem, dubbed GA-$\mathcal{H}_\infty^{\mathcal{A}}$, involves a nested three-layer optimization. It is written as

$$\max_{\boldsymbol{x}} J = \max\left(0, \gamma(\boldsymbol{\Theta}_{\mathcal{A}}^\star) - \bar{\gamma}\right) + \sum_{j=1}^{n} \max\left(0, \Sigma_j(\boldsymbol{\Theta}_{\mathcal{A}}^\star)\right) \quad (39)$$

with

$$\begin{aligned} &\boldsymbol{\Theta}_{\mathcal{A}}^\star \\ &= \arg\min_{\boldsymbol{\Theta}_{\mathcal{A}}} \max_{\Delta} \|T_{w\to z}(M_W, K(\boldsymbol{\Theta}_{\mathcal{A}}))\|_\infty \\ &\quad \text{subject to } K(\boldsymbol{\Theta}_{\mathcal{A}}) \in \mathcal{K} \quad \text{closed-loop stabilizing} \end{aligned} \quad (40)$$

where M_W is a short-hand form to remark the dependence of $M = F_u(P, \Delta)$ on the weighting functions $\boldsymbol{W}^{\text{in}}$ and $\boldsymbol{W}^{\text{out}}$. The augmented vector of tunable gains $\boldsymbol{\Theta}_{\mathcal{A}}$, that also includes the damping coefficients in the denominators of $H_N(s)$, is

$$\begin{aligned} \boldsymbol{\Theta}_{\mathcal{A}} = [&K_{P_\theta}\ K_{D_\theta}\ K_{P_Z}\ K_{D_Z} \\ &\zeta_{N1}\ \zeta_{N2}\ \zeta_{N3}\ \zeta_{D1}\ \zeta_{D2}\ \zeta_{D3}]^T \end{aligned} \quad (41)$$

The larger number of optimally tuned parameters should improve the controller capability of dealing with (possibly severe) uncertainty on the BM frequency while, as a drawback, increasing the complexity of the $\mathcal{H}_\infty$ optimization problem. Also, by considering the max of $\|\boldsymbol{T}_{w\to z}\|_\infty$ over all possible scattered conditions, this design aims at maximizing the performance over the worst-case condition from the set Δ.

For the GA-$\mathcal{H}_\infty^{\mathcal{A}}$ design procedure, the weights related to lateral drift, $W_{Z_{ins}}$ and $W_{\dot{Z}_{ins}}$, are adjusted to deal with the large uncertainty range considered in the optimization process. More precisely, for the load-relief mode the values $D_{Z_{ins}} = 2500\,\text{m}$ and $D_{\dot{Z}_{ins}} = 15\,\text{m/s}$ are used, so as to allow the algorithm to trade-off some drift performance for a reduction of the aerodynamic load $Q\alpha$. The other weights are fixed at the same values of the GA-$\mathcal{H}_\infty$ problem.

TABLE 7. Stability margins at $t = 72$ s.

Controller	Rigid-body margins			Elastic mode margins		
	Aero GM	Rigid PM	Rigid GM	Flex GM	Flex PM_1	Flex PM_2
BC	6.8 dB	109 ms	6.55 dB	18.0 dB	242 ms	127 ms
$\mathcal{H}_\infty$	6.8 dB	100 ms	6.35 dB	18.0 dB	241 ms	125 ms
GA-$\mathcal{H}_\infty$	6.1 dB	105 ms	6.43 dB	17.5 dB	250 ms	120 ms
GA-$\mathcal{H}_\infty^{\mathcal{A}}$	7.4 dB	103 ms	6.00 dB	15.5 dB	253 ms	133 ms

VI. RESULTS AND DISCUSSION

Performances of the hybrid controllers developed according to GA-$\mathcal{H}_\infty$ and GA-$\mathcal{H}_\infty^{\mathcal{A}}$ methodologies are assessed in this Section, with reference to the BC and $\mathcal{H}_\infty$ designs. The major objective is to evaluate, using the LV model discussed in Section II, possible improvements due the GA-based syntheses in terms of robust stability and performance with respect to the manually tuned controllers, also including consideration of reduced workload associated to the automated design procedures.

Preliminary runs of the GA in nominal conditions at maximum dynamic pressure led to a suitable tuning of the hyperparameters [36], as reported in Table 5. The same set of specifications and values is used for all design points.

The synthesis of GA-$\mathcal{H}_\infty$ controller requires solving the optimization problem in Eqs. (36) and (37), which takes about 18 min per design point on a computer with an Intel Core i7-4710HQ CPU @3.60 GHz 8 parallel threads and a 16 GB RAM memory. On the other hand, computer time for the GA-$\mathcal{H}_\infty^{\mathcal{A}}$ optimization (Eqs. (39) and (40)) increases to about 40 min due to the additional burden of the augmented (or worst-case) $\mathcal{H}_\infty$ optimization. In both cases, the computational time is slightly reduced when the drift-minimum mode is dealt with, where the stability constraints are somewhat relaxed and the convergence is smoother.

Lower and upper bounds that define the search space $\mathcal{X}$ of design parameters for GA-$\mathcal{H}_\infty$ and GA-$\mathcal{H}_\infty^{\mathcal{A}}$ problems are shown in Table 6. They are specified so as to avoid weighting functions with unstable poles or right-half-plane zeros, as well as non-physical functions having, for instance, negative crossover frequencies. In particular, W_{θ_e} and $W_{\theta_{ins}}$ are constrained to behave as low- and high-pass filters, respectively.

Robust stability of GA-based controllers with respect to the expected variations of model parameters (see Table 1) is evaluated first. To this end, Fig. 10 shows the upper bound of the structured singular value μ [40] at the design points, in the frequency range of interest. Distance of μ from unity provides a measure of the robustness of the controller, so that, when a curve is always below unity, stability under any possible combination of parameter uncertainties is guaranteed. It is apparent that GA-$\mathcal{H}_\infty$ and GA-$\mathcal{H}_\infty^{\mathcal{A}}$ controllers are both robustly stable, the latter showing improved margins as the distance from unity is slightly larger than in the case of GA-$\mathcal{H}_\infty$.

Figure 11 presents the Nichols plots of the open-loop response for the four controllers, evaluated in nominal

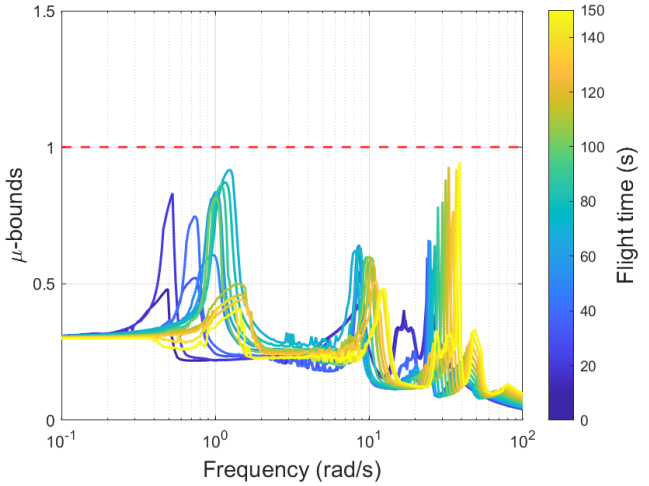

(a) GA-$\mathcal{H}_\infty$

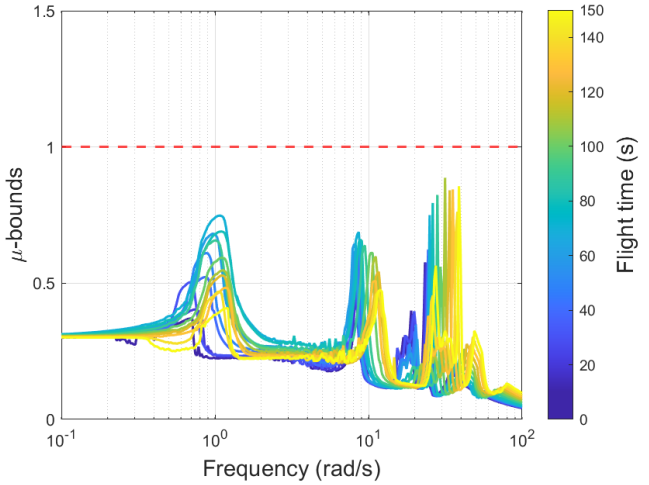

(b) GA-$\mathcal{H}_\infty^{\mathcal{A}}$

FIGURE 10. Robust stability of GA-$\mathcal{H}_\infty$ and GA-$\mathcal{H}_\infty^{\mathcal{A}}$ controllers vs. frequency at design points.

condition at $t = 72$ s. The related stability margins, shown in Table 7, are somewhat similar for all controllers, with a major difference concerning the low-frequency Aero GM and Rigid GM. Note that BC tuning allows to achieve a condition where both margins are larger than the requirement (6 dB) and close to each other. This is not the case for the GA-$\mathcal{H}_\infty^{\mathcal{A}}$ controller, where the optimization pushes the margins toward, respectively, a maximum (Aero GM = 7.4 dB) and a minimum (Rigid GM = 6.0 dB), resulting in a more robust design at low frequency, as visible in Fig. 10 when the μ-bounds at frequencies below 8 rad/s are compared.

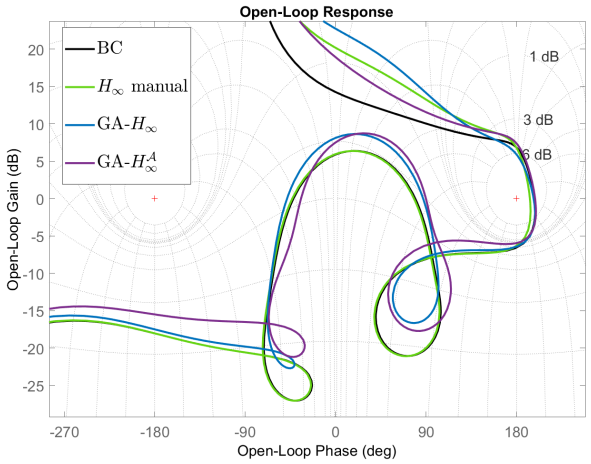

FIGURE 11. Comparison of Nichols plots of open-loop response, $t = 72$ s.

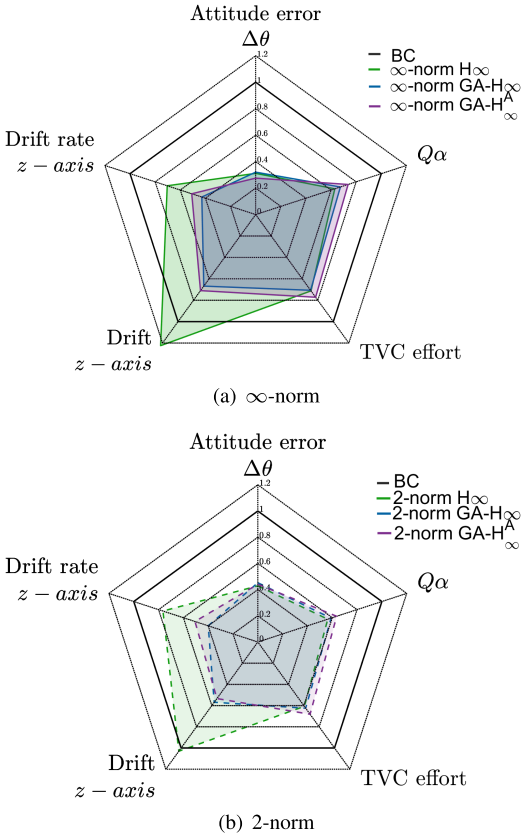

FIGURE 12. MC1: radar chart of the normalized controller performances.

Conversely, the GA-$\mathcal{H}_\infty$ controller, presents a lower value of Aero GM (6.1 dB), since the optimization primarily aims at maximizing the performance in nominal conditions, while the stability requirement on GMs is less relevant. In this respect, the distance of μ-bounds from unity is slightly lower than in GA-$\mathcal{H}_\infty^{\mathcal{A}}$, which indicates that the controller will be somewhat less robust to off-nominal scattering conditions.

Finally, note that the GA-based controllers, that take advantage of a highly automated design process, are able to retain the stability performance of $\mathcal{H}_\infty$, the synthesis of which may result in a cumbersome process that requires a sound knowledge on LV dynamic behaviour, together with experience on suitability and effectiveness of guidelines currently adopted for tuning the weighting functions.

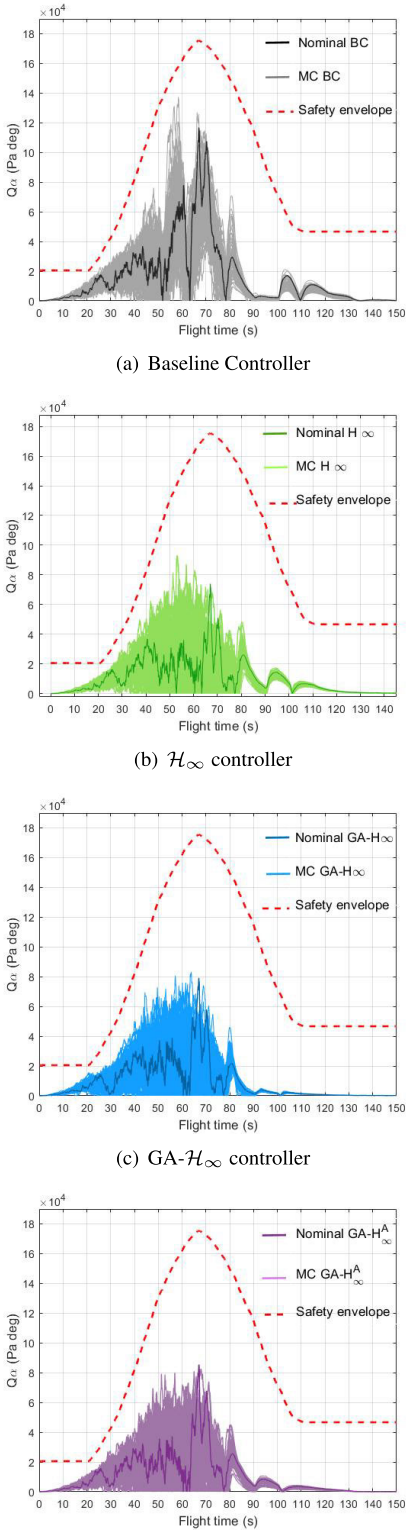

FIGURE 13. MC1: aerodynamic load response vs. flight time for the four controllers; bold continuous lines indicate no scattering.

In order to further investigate the performances of hybrid designs, a Monte Carlo campaign of 2.000 runs, dubbed MC1, is carried out, with parameters of the LV model scattered as reported in Table 1, and severe wind disturbances (see Eq. (16)–(17)), For each simulation the figures of merit of attitude error ($\Delta\theta$, drift (z) and drift-rate ($\dot{z}$) along the lateral axis, TVC effort, and aerodynamic bending load ($Q\alpha$) are evaluated. Figure 12 shows the ∞-norm and 2-norm of the metrics, related to maximum value and energy, respectively, averaged over all runs and normalized with respect to the same quantities computed for the BC. It is apparent that performances of GA-tuned controllers are close to that of the $\mathcal{H}_\infty$, and significantly improved in comparison to BC in terms of both norms. In particular, GA-$\mathcal{H}_\infty^{\mathcal{A}}$ reduces the attitude error of 72%, and peak drift and drift rate of about 29% and 49%, respectively, while requiring a lower control effort (about -22%). The aerodynamic load $Q\alpha$ is decreased by about 25%. Also, the GA-based controllers allow for a further reduction of the lateral drift and drift rate with respect to the $\mathcal{H}_\infty$ design, at the expense of a slightly larger control effort.

A second Monte Carlo campaign, referenced as MC2, is conducted using the same variation of LV model parameters already considered in MC1, and a single wind profile so as to improve clarity in the analysis of the effects of parameter scattering on the aerodynamic load $Q\alpha$ once the wind data dispersion is removed. Figure 13 reports the time histories of $Q\alpha$ for all controllers, together with the related safety envelope (dashed line) and the results obtained in the nominal condition, that is, with no scattering. When comparing the envelope of the $Q\alpha$ curves in Fig. 13(a), which refers to the BC, with the results of the three $\mathcal{H}_\infty$-based controllers in Figs. 13(b)–13(d) the advantage of using the robust control design framework is apparent. In particular, a reduction of about 35% in the maximum $Q\alpha$ peak is obtained when using GA-$\mathcal{H}_\infty^{\mathcal{A}}$ in place of BC. It is also worth to mention that the robust controllers behave very closely in terms of $Q\alpha$ reduction, with GA-$\mathcal{H}_\infty^{\mathcal{A}}$ providing a slightly better performance over the $\mathcal{H}_\infty$ and GA-$\mathcal{H}_\infty$ designs, as reductions of the peak value of $Q\alpha$ of about 8 and 3% are obtained.

The second Monte Carlo campaign confirms the results obtained in MC1 on the viability of the GA-based tuning methodology, and its ability to produce controller that recover and possibly improve the robust performance provided by the structured $\mathcal{H}_\infty$ synthesis.

VII. CONCLUSION

In this paper a novel approach to the automated synthesis of the flight control system (FCS) for a launch vehicle (LV) in atmospheric flight has been presented. It relies on a hybrid design methodology where an optimization problem is formulated and solved by a genetic algorithm (GA) in order to determine the weighting function coefficients of a controller synthesized by the structured $\mathcal{H}_\infty$ technique. The aim is to reduce the design effort while guaranteeing performance and robustness characteristics equal or superior to those achieved by more classic approaches in LV FCS development.

Two design techniques, dubbed GA-$\mathcal{H}_\infty$ and GA-$\mathcal{H}_\infty^{\mathcal{A}}$ have been proposed. The former considers a nested, two-level optimization problem, where the GA searches for the input/output weights so as to guarantee compliance with some assigned high-level requirements, expressed in terms of linear stability margins. The GA-$\mathcal{H}_\infty^{\mathcal{A}}$ can be regarded as a logical extension of GA-$\mathcal{H}_\infty$, where advantage is taken from a linear fractional transformation (LFT) based LV model with structured uncertainty, in order to bring into the optimization process the information on the envisioned ranges of parameter variations.

Extended simulation campaigns were carried out in realistic operating scenarios, considering wide ranges of scattering for model parameters and external disturbances, according to standard procedures for LV control system validation and verification. The results show that the nested-optimization methodology provides a streamlined procedure for the synthesis of robustly stable controllers, that satisfy the desired requirements, and may reduce the burden of design, tuning and validation procedures associated to more traditional design methods. The latter advantage depends on the high level of automation in the proposed procedure, where the parameters of weighting functions for the $\mathcal{H}_\infty$ synthesis are obtained by the solution of an optimization problem. It is to be remarked that the GA-$\mathcal{H}_\infty$ technique is able to devise a controller with performance comparable or even superior to the structured $\mathcal{H}_\infty$ synthesis, in a relatively small amount of time, while requiring only a minimal knowledge about LV system.

Similar results are obtained using the GA-$\mathcal{H}_\infty^{\mathcal{A}}$ approach, that is more computationally intensive (about twice CPU-time), but leads to a controller that, as said, is robust by design to any combination of the considered scattering of model parameters. In the present application, the stability margins obtained by the GA-$\mathcal{H}_\infty^{\mathcal{A}}$ synthesis are close to those of the other controllers. This is probably due to the fact that requirements are rather conservative, so that stability is always guaranteed for the considered level of model uncertainty.

The GA-$\mathcal{H}_\infty$ controller appears as the best trade-off in terms of performance, robustness, and workload for tuning, showing no drawbacks or limitations with respect to the structured $\mathcal{H}_\infty$ methodology. Application of the GA-$\mathcal{H}_\infty^{\mathcal{A}}$ approach is expected to be more promising for future LVs where, due to tighter constraints on cost and growing expectations on vehicle performance, parameter uncertainties and model errors could be potentially larger with respect to the actual systems, and the definition of requirement for control synthesis might not be trivial.

The enhanced level of robustness and the automated tuning process associated to GA-$\mathcal{H}_\infty$ and GA-$\mathcal{H}_\infty^{\mathcal{A}}$ might be of interest from an industrial perspective in order to simplify the engineering task of FCS design across multiple missions, particularly when cost and time of the recurrent activities of

mission integration and flight program software validation and verification, taking place before each new launch, are taken into consideration. On the other hand, some drawbacks of the methodology should be addressed in order to improve control system performance, and/or make more effective the design procedure. In this respect, a viable and more general methodology for the definition of performance metrics so as to achieve full compliance with requirements should be developed. Also, a systematic methodology for the selection of the bounds of weighting function coefficients, that significantly influence the convergence characteristics of the GA solver, could be devised.

In future developments of the study, the analysis of controllers synthesized according to the proposed methodology will be carried on a high-fidelity LV model featuring, among other effects neglected in the present application, nonlinear actuator dynamics, coupling of pitch and yaw dynamics, and higher-order flexible modes.

REFERENCES

[1] D. Garner, "Control theory handbook," NASA Marshall Space Flight Center, Huntsville, AL, USA, Tech. Rep. NASA TM-X-53036, 1964.
[2] A. L. Greensite, "Analysis and design of space vehicle flight control systems. Volume VII-Attitude control during launch," NASA Marshall Space Flight Center, Huntsville, AL, USA, Tech. Rep. NASA-CR-826, GD/C-DDE66-028, 1967.
[3] J. Hanson, "A plan for advanced guidance and control technology for 2nd generation reusable launch vehicles," in *Proc. AIAA Guid., Navigat., Control Conf. Exhib.*, Aug. 2002, p. 4557.
[4] K. J. Astrom and B. Wittenmark, *Adaptive Control*, 2nd ed. Reading, MA, USA: Addison-Wesley, 1994.
[5] P. Parks, "Liapunov redesign of model reference adaptive control systems," *IEEE Trans. Autom. Control*, vol. AC-11, no. 3, pp. 362–367, Jul. 1966.
[6] S. Creech, T. May, and K. Robinson, "NASA's space launch system: An enabling capability for international exploration," in *Proc. IAA Space Explor. Conf.*, Washington, DC, USA, 2014, pp. 1–11.
[7] J. Orr and T. Van Zwieten, "Robust, practical adaptive control for launch vehicles," in *Proc. AIAA Guid., Navigat., Control Conf.*, Aug. 2012, p. 4549.
[8] J. H. Wall, J. S. Orr, and T. S. VanZwieten, "Space launch system implementation of adaptive augmenting control," in *Proc. 37th Annu. Amer. Astron. Soc. (AAS) Guid., Navigat., Control Conf.*, Breckenridge, CO, USA, 2014, pp. 1–16.
[9] D. Trotta, A. Zavoli, G. De Matteis, and A. Neri, "Opportunities and limitations of adaptive augmented control for launch vehicle attitude control in atmospheric flight," in *Proc. Astrodynamics Spec. Conf.*, Portland, Maine, Aug. 2019, pp. 11–15.
[10] T. S. VanZwieten, M. R. Hannan, and J. H. Wall, "Evaluating the stability of NASA's space launch system with adaptive augmenting control," *CEAS Space J.*, vol. 10, no. 4, pp. 583–595, Dec. 2018.
[11] J. C. Doyle, K. Glover, P. P. Khargonekar, and B. A. Francis, "State-space solutions to standard H_2 and H_∞ control problems," *IEEE Trans. Autom. Control*, vol. 34, no. 8, pp. 831–847, Aug. 1989.
[12] C. Roux and I. Cruciani, "Scheduling schemes and control law robustness in atmospheric flight of VEGA launcher," in *Proc. 7th ESA GNC Conf.*, 2008, pp. 1–5.
[13] A. P. White, G. Zhu, and J. Choi, *Linear Parameter-Varying Control for Engineering Applications*. London, U.K.: Springer-Verlag GmbH, 2013.
[14] M. Ganet and M. Ducamp, "LPV control for flexible launcher," in *Proc. AIAA Guid., Navigat., Control Conf.* Reston, VA, USA: American Institute of Aeronautics and Astronautics, Aug. 2010, pp. 1–19.
[15] P. Gahinet and P. Apkarian, "Structured H∞ synthesis in MATLAB," *IFAC Proc. Volumes*, vol. 44, no. 1, pp. 1435–1440, Jan. 2011.
[16] M. Ganet-Schoeller and J. Desmariaux, "Structured H∞ synthesis for flexible launcher control," *IFAC-PapersOnLine*, vol. 49, no. 17, pp. 450–455, 2016.
[17] D. Navarro-Tapia, A. Marcos, S. Bennani, and C. Roux, "Robust-control-based design and comparison of an adaptive controller for the VEGA launcher," in *Proc. AIAA Scitech Forum*. Reston, VA, USA: American Institute of Aeronautics and Astronautics, Jan. 2019, pp. 1–14.
[18] K. Krishnakumar and D. E. Goldberg, "Control system optimization using genetic algorithms," *J. Guid., Control, Dyn.*, vol. 15, no. 3, pp. 735–740, May 1992, doi: 10.2514/3.20898.
[19] A. Jayachitra and R. Vinodha, "Genetic algorithm based PID controller tuning approach for continuous stirred tank reactor," *Adv. Artif. Intell.*, vol. 2014, pp. 1–8, Dec. 2014.
[20] R. Fantinutto, G. Guglieri, and F. B. Quagliotti, "Flight control system design and optimisation with a genetic algorithm," *Aerosp. Sci. Technol.*, vol. 9, no. 1, pp. 73–80, Jan. 2005. [Online]. Available: https://www.sciencedirect.com/science/article/pii/S1270963804001117
[21] Z. He and L. Zhao, "A simple attitude control of quadrotor helicopter based on Ziegler-Nichols rules for tuning PD parameters," *Sci. World J.*, vol. 2014, pp. 1–13, Dec. 2014.
[22] D. Trotta, G. D. Matteis, A. Zavoli, and V. D'Antuono, *Optimal Tuning for Robust Control of a Small Fixed-Wing UAV*. Reston, VA, USA: American Institute of Aeronautics and Astronautics, 2021, doi: 10.2514/6.2021-1057.
[23] H.-G. Beyer and B. Sendhoff, "Robust optimization—A comprehensive survey," *Comput. Methods Appl. Mech. Eng.*, vol. 196, nos. 33–34, pp. 3190–3218, Jul. 2007.
[24] D. Trotta, A. Zavoli, G. D. Matteis, and A. Neri, "Optimal tuning of adaptive augmenting controller for launch vehicles in atmospheric flight," *J. Guid., Control, Dyn.*, vol. 43, no. 11, pp. 1–8, 2020.
[25] D. Navarro-Tapia, A. Marcos, S. Bennani, and C. Roux, "Joint robust structured design of VEGA launcher's rigid-body controller and bending filter," in *Proc. 69th Int. Astron. Congr.*, vol. 1, 2018, pp. 7980–7993.
[26] G. Balas, J. C. Doyle, K. Glover, A. Packard, and R. smith, *μ-Analysis and Synthesis Toolbox*. Portola Valley, CA, USA: MathWorks, 1993.
[27] A. L. Greensite, "Analysis and design of space vehicle flight control systems. Volume XV-Elastic body equations," NASA Marshall Space Flight Center, Tech. Rep. NASA-CR-834, GD/C-DDE65-025, 1967.
[28] D.-W. Gu, P. H. Petkov, and M. M. Konstantinov, *Robust Control Design With MATLAB*. London, U.K.: Springer-Verlag GmbH, 2013.
[29] D. Johnson, "Terrestrial environment (climatic) criteria guidelines for use in aerospace vehicle development. 2008 revision," NASA, Washington, DC, USA, Tech. Rep. NASA/TM 2008-215633, 2008.
[30] B. Wie and K.-W. Byun, "New generalized structural filtering concept for active vibration control synthesis," *J. Guid., Control, Dyn.*, vol. 12, no. 2, pp. 147–154, Mar. 1989.
[31] I. P. S. Skogestad, *Multivariable Feedback Control*. John Hoboken, NJ, USA: Wiley, 2005.
[32] W. M. Lu, K. Zhou, and J. C. Doyle, "Stabilization of uncertain linear systems: An LFT approach," *IEEE Trans. Autom. Control*, vol. 41, no. 1, pp. 50–65, Jan. 1996.
[33] A. M. Simoes, D. C. Savelli, P. C. Pellanda, N. Martins, and P. Apkarian, "Robust design of a TCSC oscillation damping controller in a weak 500-kV interconnection considering multiple power flow scenarios and external disturbances," *IEEE Trans. Power Syst.*, vol. 24, no. 1, pp. 226–236, Feb. 2009.
[34] D. Navarro-Tapia, A. Marcos, P. Simplício, S. Bennani, and C. Roux, "Legacy recovery and robust augmentation structured design for the VEGA launcher," *Int. J. Robust Nonlinear Control*, vol. 29, no. 11, pp. 3363–3388, Jul. 2019.
[35] J. E. Bibel and D. S. Malyevac, "Guidelines for the selection of weighting functions for H-infinity control," Nav. Surface Warfare Center, Dahlgren, VA, Tech. Rep. NSWCDD/MP-92/43, 1992.
[36] M. Mitchell, *An Introduction to Genetic Algorithms* (Complex Adaptive Systems). Cambridge, MA, USA: MIT Press, 1998.
[37] K. Deb and R. B. Agrawal, "Simulated binary crossover for continuous search space," *Complex Syst.*, vol. 9, no. 2, pp. 115–148, 1995.
[38] A. Hassanat, K. Almohammadi, E. Alkafaween, E. Abunawas, A. Hammouri, and V. B. S. Prasath, "Choosing mutation and crossover ratios for genetic Algorithms—A review with a new dynamic approach," *Information*, vol. 10, no. 12, p. 390, Dec. 2019.
[39] P. Apkarian, M. N. Dao, and D. Noll, "Parametric robust structured control design," *IEEE Trans. Autom. Control*, vol. 60, no. 7, pp. 1857–1869, Jul. 2015.
[40] A. Packard and J. Doyle, "The complex structured singular value," *Automatica*, vol. 29, no. 1, pp. 71–109, Jan. 1993.

JOSÉ PABLO BELLETTI ARAQUE was born in Santiago, Chile, in 1989. He received the B.S. degree in aerospace engineering and the M.S. degree in aeronautical engineering from the Sapienza University of Rome. He is currently a Research Fellow with the Department of Mechanical and Aerospace Engineering, Sapienza University of Rome. He is also working as an Aeronautical Engineer with the Space and Defense Industry. His main research interests include flight dynamics of aerospace vehicles and flight control system applications. He is also involved in the development of robust control systems for launch vehicles in atmospheric flight, aircrafts and missile application as well guidance methods for missile systems for mid-course and terminal phase.

ALESSANDRO ZAVOLI was born in Rimini, Italy, in 1985. He received the B.S. degree in aerospace engineering and the M.S. degree in space engineering from the Sapienza University of Rome, and the Ph.D. degree in aeronautical and space technologies from the Sapienza University of Rome, in 2013. He is currently a Research Assistant with the Department of Mechanical and Aerospace Engineering, Sapienza University of Rome. His research interests include spacecraft trajectory optimization, where he focused on the application of indirect methods for interplanetary mission design and ascent trajectory optimization. He participated to several edition of the Global Trajectory Optimization Competition, most notably the 6th edition in 2012, where his team ranked first. Since 2014, his research also encompasses spacecraft attitude control. His study concerns the analysis and synthesis of nonlinear controls for underactuated systems, such as magnetically actuated spacecraft. He is also involved in support and cross-check activities for ESA-ESRIN in the framework of VEGA launch vehicle program, investigating modern optimization methods and robust and adaptive control laws for atmospheric flight.

DOMENICO TROTTA received the B.S. degree in aerospace engineering and the M.S. degree in aeronautical engineering from the Sapienza University of Rome, and the Ph.D. degree in aeronautical and space technologies from the Sapienza University of Rome, in 2021. He is currently a Research Fellow with the Department of Mechanical and Aerospace Engineering, Sapienza University of Rome. His research interests include the flight dynamics and control techniques for autonomous aerospace vehicles. He is also involved in the development of adaptive control techniques for the attitude control launch vehicles in atmospheric flight in order to increase flight control system robustness in the presence of uncertain vehicle parameters.

GUIDO DE MATTEIS is currently a Professor of flight mechanics with the University of Rome ''La Sapienza,'' where he teaches the courses of flight dynamics and helicopter flight mechanics. The principal fields of research are in the dynamics and control of spacecraft, transatmospheric vehicles and aircraft. He is also doing researches on spacecraft attitude dynamics and control, modeling and control of launch vehicles, inverse simulation of rotorcraft dynamics, development of guidance and control laws for remotely piloted vehicles, with focus on real-time, hardware-in-the-loop simulation for control system validation and/or handling qualities evaluation. He is also the Head of the Flight Dynamics Laboratory, Department of Mechanical and Aerospace Engineering, dedicated to design and development of research UAVs, and flight simulation of aerospace vehicles.